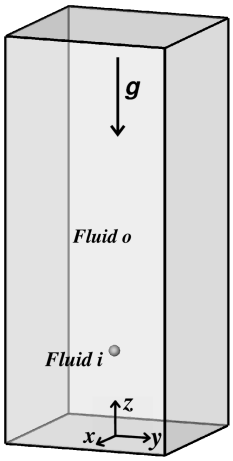

Supplementary Figure 1. Three dimensional domain for the numerical simulation. Schematic diagram showing the initial configuration of a bubble (fluid 'i') rising in a far denser and more viscous fluid (fluid 'o') under the action of gravity, which is acting in the negative z direction. A computational domain of size $(L, W, H) = (30R, 30R, 120R)$, given in x, y and z respectively, is considered in this study, where R is the radius of the bubble. Note that $L = W$ in all the computations. Initially the bubble is located at $(0, 0, 8R)$.

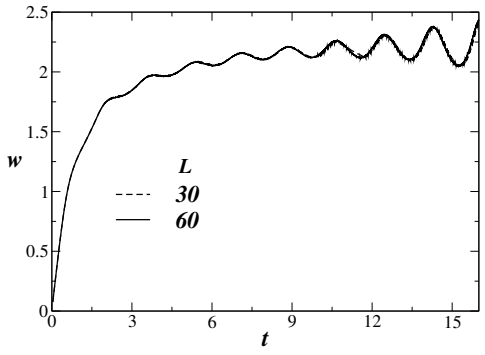

Supplementary Figure 2. Effect of domain size on axial velocity of a bubble exhibiting a spiralling motion. The parameter values are $Ga = 100$ and $Eo = 0.5$.

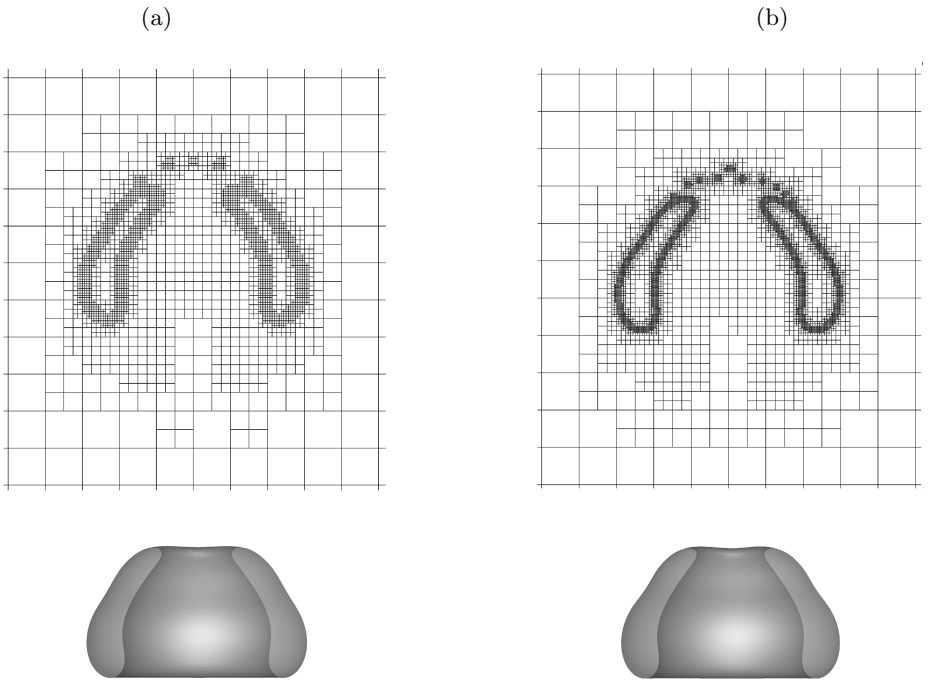

Supplementary Figure 3. Effect of grid size on the simulation results. The shapes of the bubble for two different grids at $t = 3$ is shown. The parameter values are $Ga = 70.7$ and $Eo = 200$. The smallest grid size in panels (a) and (b) are about 0.029 and 0.014, respectively.

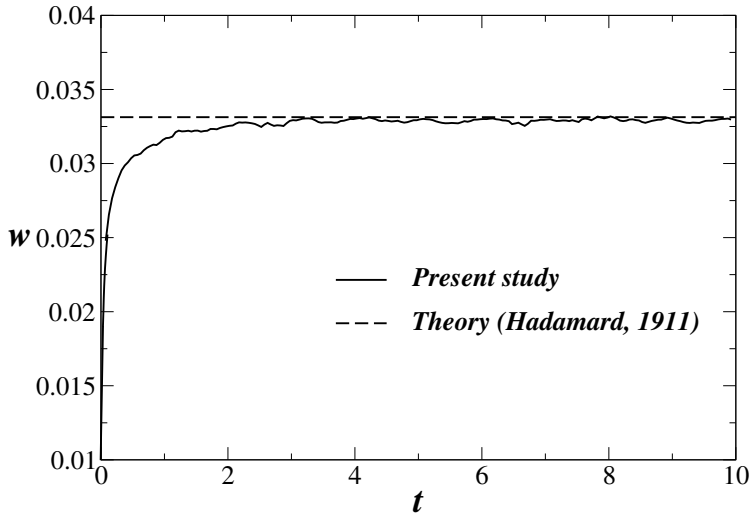

Supplementary Figure 4. Comparison of present numerical result with Hadamard-Rybczynski [11] theory. The terminal velocity agrees well for a domain size of $30 \times 30 \times 120$ and for the parameter values: $Ga = 0.1$ and $Eo = 0.1$.

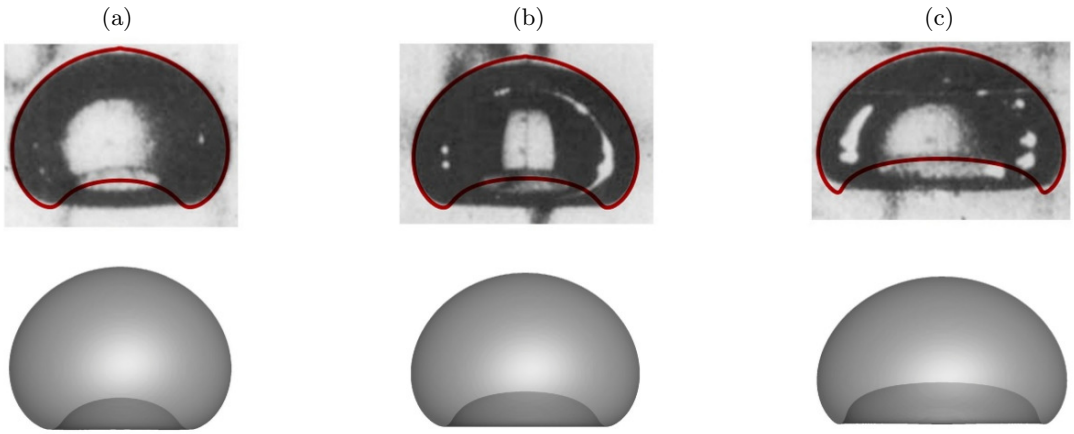

Supplementary Figure 5. Comparison of terminal shape of the bubble with the results of Bhaga & Weber [13]. The parameter values are: (a) $Ga = 2.316, Eo = 29$, (b) $Ga = 3.094, Eo = 29$, and (c) $Ga = 4.935, Eo = 29$. The photographs in the top row are reproduced from Bhaga & Weber [13], and the results in the bottom row are obtained from the present three-dimensional simulations. The results from the corresponding axisymmetric simulations are shown by red lines in the top row.

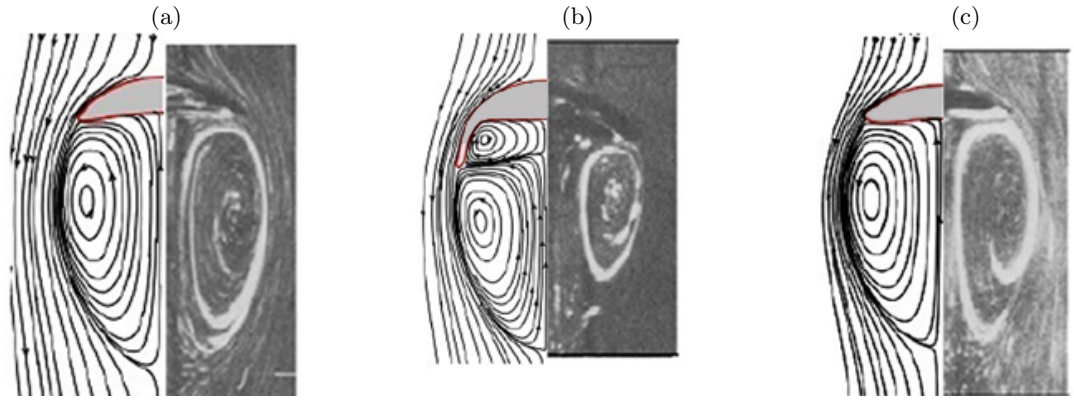

Supplementary Figure 6. Comparison of the streamline patterns with those obtained by Bhaga & Weber [13]. The parameter values are: (a) $Ga = 40.54, Eo = 23.57$, (b) $Ga = 24.72, Eo = 37.75$, and (c) $Ga = 46.11, Eo = 15.47$. The results from our axisymmetric simulations are shown on the left half and the results reproduced from Bhaga & Weber [13] are shown on the right half of each subfigure.

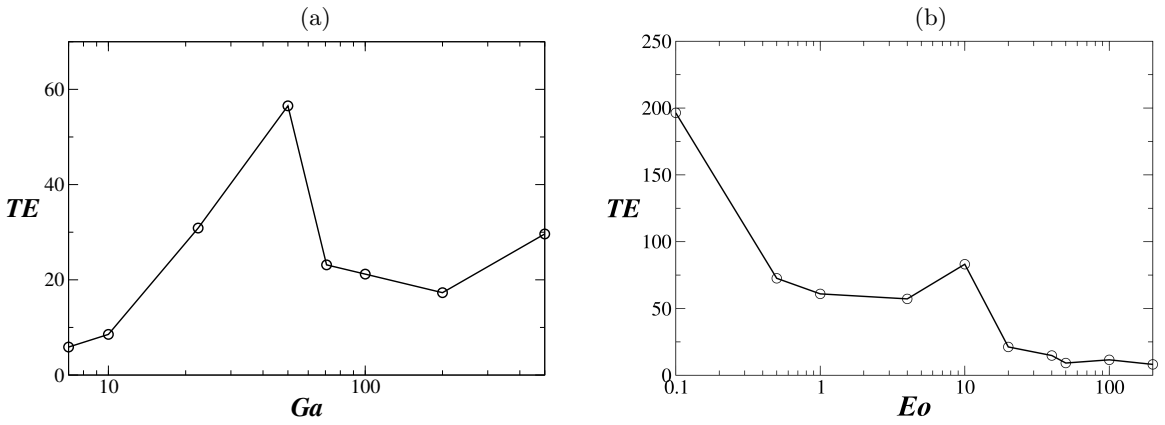

Supplementary Figure 7. Variation of the sum of kinetic and surface energies with Ga and Eo. The parameter values are: (a) $Eo = 20$, and (b) $Ga = 100$.

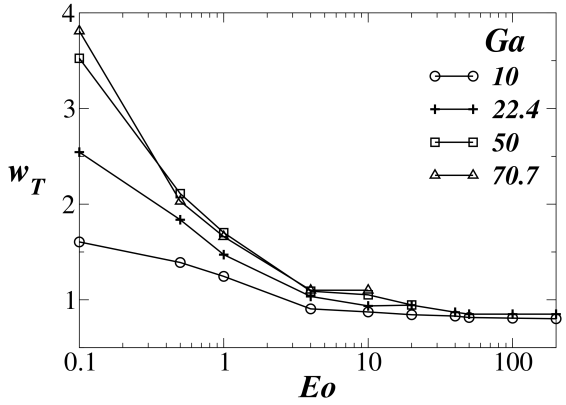

Supplementary Figure 8. Variation of the dimensionless terminal velocity with Eo for different values of Ga.

Supplementary Note 1: Effect of domain size

The effect of domain size is investigated (see supplementary figure 2), where the axial rise velocity of the spiralling bubbles is plotted versus time for two different values of dimensionless L. It is found that doubling the size of the lateral cross-section of the domain (i.e doubling L and W) has a negligible effect (less than 0.2% on the rise velocity as shown in the supplementary figure 2) on the flow dynamics. We found that the shapes of the bubble for both the cases are indistinguishable. In addition to this, it is to be noted here that [9] and [10] considered L to be about 30 in their experimental and numerical studies of the path instability of rising bubble, and fragmentation process of a falling drop, respectively. Thus a computational domain $30 \times 30 \times 120$ is used in the present study. All lengths are scaled by the radius of the bubble.

Supplementary Note 2: Grid convergence test

As mentioned in the main manuscript, the dynamic adaptive grid refinement feature of Gerris has been employed to refine the grid at the interface and in the regions where a relatively greater magnitude of vorticity is present. This ensures, in addition to an accurate advection of the interface, that the flow field is resolved in the regions of the domain where the gradients in velocity are large. These two refinement criteria are visible in the supplementary figure 3. The coarsest refinement level used in our simulations is 6 which corresponds to 64 computational cells per unit domain width, and the finest level being 10 near the interface, which amounts to 1024 computational cells per unit domain width. An intermediate refinement of 256 cells per unit domain width is used for regions with a significant amount of vorticity magnitude. In the supplementary figure 3 we show bubble shapes obtained using two different grids. It reveals that grid convergence is achieved for simulations having the smallest grid less than 0.029. This means that we have about 70 grid points across a vertical bubble cross section.

Supplementary Note 3: Comparison with theory

The analytical studies of Hadamard [11] and Rybczinsky [12] were the first to derive the flow field in a slowly rising/falling spherical blob of a fluid in another fluid. The expression of theoretical rise velocity, from these studies, can be expressed in terms of our diemnsionless variables as

$$w_T = \frac{2Ga(1-\rho_r)}{3}\left(\frac{1+\mu_r}{2+3\mu_r}\right).$$

In order to investigate the effect of domain size for a difficult case (i.e for very low value of Ga), the rise velocity obtained from the present numerical solver are plotted against time in the supplementary figure 4 for $Ga = 0.1$ and $Eo = 0.1$. An air-water system is considered for this purpose, i.e $\rho_r = 10^{-3}$ and $\mu_r = 10^{-2}$. It can be seen that the present result obtained for a domain $30 \times 30 \times 120$ (as considered in the present investigation) agrees very well with the analytically obtained terminal velocity ($w_T = 0.03313$). We also note here that the streamline patterns obtained from our simulations agree with those of Hadamard-Rybczinsky (please see Tripathi et al. [8]). This is another confirmation that the domain size used in the present study is large enough for the parameter values considered in the present investigation.

Supplementary Note 4: Comparison with experiments

Next we validated our solver by comparing with the experimental results of Bhaga & Weber [13] in the supplementary figure 5 for different values of Ga and Eo. It can be seen that the results are in good agreement. It is also noted here that the dynamics of larger bubbles are sensitive to initial conditions.

We have also performed several other validation exercises by comparing our results with previous experimental [14] and computational [15] works. For example, we have compared our results with Sussman & Smereka [16], who studied the fluid dynamics of a rising bubble displaying topology change in the framework of a level-set approach, and found excellent agreement. We refer the reader to Tripathi et al. [8] for more details. Furthermore, the present results have been compared with the streamline patterns obtained by Bhaga & Weber [13] in the Supplementary Fig. 6.

Supplementary references

[1] Popinet, S. Gerris a tree-based adaptive solver for the incompressible euler equations in complex geometries. *J. Comput. Phys* **190**, 572–600 (2003).

[2] Francois, M. M. *et al.* A balanced-force algorithm for continuous and sharp interfacial surface tension models within a volume tracking framework. *J. Comput. Phys* **213**, 141–173 (2006).

[3] Popinet, S. An accurate adaptive solver for surface-tension-driven interfacial flows. *J. Comput. Phys* **228**, 5838–5866 (2009).

[4] Herrmann, M. A balanced force refined level set grid method for two-phase flows on unstructured flow solver grids. *J. Comput. Phys* **227**, 2674–2706 (2008).

[5] Sussman, M., Smith, K. M., Hussaini, M. Y., Ohta, M. & Zhi-Wei, R. A sharp interface method for incompressible two-phase flows. *J. Comput. Phys* **221**, 469–505 (2007).

[6] Shin, S., Abdel-Khalik, S., Daru, V. & Juric, D. Accurate representation of surface tension using the level contour reconstruction method. *J. Comput. Phys* **203**, 493–516 (2005).

[7] Fuster, D., Agbaglah, G., Josserand, C., Popinet, S. & Zaleski, S. Numerical simulation of droplets, bubbles and waves: state of the art. *Fluid dynamics research* **41**, 065001 (2009).

[8] Tripathi, M. K., Sahu, K. C. & Govindarajan, R. Why a falling drop does not in general behave like a rising bubble. *Sci. Rep.* **4** (2014).

[9] Hartunian, R. A. & Sears, W. On the instability of small gas bubbles moving uniformly in various liquids. *J. Fluid Mech.* **3**, 27–47 (1957).

[10] Jalaal, M. & Mehravaran, K. Fragmentation of falling liquid droplets in bag breakup mode. *Int. J. Multiphase Flow* **47**, 115132 (2012).

[11] Hadamard, J. Mouvement permanent lent dune sphere liquide et visqueuse dans un liquide visqueux. *CR Acad. Sci* **152**, 1735–1738 (1911).

[12] Rybzynski, W. ber die fortschreitende bewegung einer flssigen kugel in einem zhen medium. *Bull. Acad. Sci.* (1911).

[13] Bhaga, D. & Weber, M. E. Bubbles in viscous liquids: shapes, wakes and velocities. *J. Fluid Mech.* **105**, 61–85 (1981).

[14] Clift, R., Grace, J. & Weber, M. *Bubbles, Drops and Particles* (Academic Press, New York, 1978).

[15] Han, J. & Tryggvason, G. Secondary breakup of axisymmetric liquid drops. i. acceleration by a constant body force. *Phys. Fluids* **11**, 3650 (1999).

[16] Sussman, M. & Smereka, P. Axisymmetric free boundary problems. *J. Fluid Mech.* **341**, 269–294 (1997).

[17] Landel, J. R., Cossu, C. & Caulfield, C. P. Spherical cap bubbles with a toroidal bubbly wake. *Phys. Fluids* **20**, 122201 (2008).